Dual-frequency narrowband CW fiber laser implementing self-injection locking of DFB laser diode and Brillouin lasing in a single ring cavity

V. V. Spirin[a], J. L. Bueno-Escobedo[a], C. A. Lopez-Mercado[a], P. Mégret[b], D. A. Korobko[c], I. O. Zolotovskii[c], A. A. Fotiadi[b,c,d]

[a]Centro de Investigación Científica y de Educación Superior de Ensenada, Carretera Ensenada-Tijuana No.3918, Zona Playitas, 22860 Ensenada, B.C., Mexico.

[b]University of Mons, Boulevard Dolez 31, 7000 Mons, Belgium.

[c]Ulyanovsk State University, 42 Leo Tolstoy Street, Ulyanovsk, 432970, Russia.

[d]Ioffe Physico-Technical Institute of the RAS, 26 Polytekhnicheskaya Street, St. Petersburg 194021, Russia.

ABSTRACT

Linewidth narrowing and stabilization of semiconductor laser light generation is of great research interest governed by the huge demand of compact cost-effective narrow-band laser sources for many potential applications. In 2012 we have demonstrated a simple kHz-linewidth laser just splicing a standard distributed feedback (DFB) laser diode and a few passive telecommunication components. The principle of operation employs the mechanism of self-injection locking that significantly improves DFB laser performance. While a typical linewidth of free-running DFB semiconductor lasers ranges from a few to tens MHz, self-injection locking of a DFB laser through an external fiber ring cavity causes a drastic reduction of its laser linewidth down to a few kHz. The advantage of the proposed configuration is that the same external fiber ring cavity could be used for self-injection locking of a DFB laser and as Brillouin scattering media to generate Stokes shifted optical wave. However, a continuous laser operation at two frequencies has not been reported yet preventing it from many prosperous photonic applications. Here, we introduce a simple dual-frequency laser configuration. In our approach, the implementation of self-injection locking into the Brillouin ring fiber laser helps to maintain coupling between the DFB laser and an external high-Q fiber cavity enabling dual-frequency laser operation. Specifically, the same ring fiber cavity is used to generate narrow-band light at the pump frequency (through self-injection locking mechanism) and narrow-band laser light at Stokes frequency (through stimulated Brillouin scattering). The system is supplied by a low-bandwidth active optoelectronic feedback circuit controlled by a low-cost USB-DAQ card that helps the laser to maintain the desired operation mode. The fiber configuration reduces the natural Lorentzian linewidth of light emitted by the laser at pump and Stokes frequencies down to 270 Hz and 220 Hz, respectively, and features a stable 300-Hz-width RF spectrum recorded with the beating of two laser outputs. We have explored key features of the laser performance, revealing its stability and applicability to RF harmonic generation of high spectral purity as an additional benefit of the proposed technique.

Keywords: narrowband laser sources; self-injection locking; Brillouin lasing.

1. INTRODUCTION

Linewidth narrowing and stabilization of semiconductor laser light generation is of great research interest governed by a huge demand of compact cost-effective narrow-band laser sources for many potential applications [1-13]. In 2012 we have demonstrated a simple kHz-linewidth laser just splicing a standard DFB laser diode and a few passive telecommunication components [14]. The principle of operation employs the mechanism of self-injection locking that significantly improves the DFB laser performance [15-20]. While a typical linewidth of free-running DFB semiconductor lasers ranges from a few to tens MHz, self-injection locking of the DFB laser through an external fiber ring cavity causes a drastic reduction of the laser linewidth down to a few kHz. The main drawback of this technique is its high sensitivity to fluctuations of the configuration parameters and surroundings.

Several approaches have been performed to stabilize the laser operation in the self-injection locking regime [21-30]. Once getting locking to the cavity resonance, the laser starts to generate the cavity resonant frequency. Then any slow change of the ring mode frequency (due to environment temperature fluctuations, for example) near the stability point causes the same change of the laser frequency. However, a more extended drift of the cavity mode frequency (>10 MHz) causes mode-hopping making laser operation temporally unstable. In our previous experiments, a stable laser operation has been commonly observed for a few seconds. With precise stabilization of the laser diode current and temperature applied in conjugation with the thermal control of the whole fiber configuration this time could be extended to tens of minutes and even more [31]. However, these stabilization solutions are technically complicated and rather costly.

An alternative solution has been proposed recently [32, 33]. We have demonstrated stabilization of semiconductor DFB laser in self-injection locking regime implementing an active optoelectronic feedback circuit controlled by a low-cost USB-DAQ card. In this approach, the narrowing of DFB laser linewidth is still provided by the self-injection-locking mechanism, whereas the active feedback is used to maintain the laser operation in this regime. Therefore, in terms of feedback circuit bandwidth, complexity, and allocated memory, this method is much less consuming than optoelectronic systems commonly used with fiber lasers [34, 35]. An advance of the proposed configuration is that the same external fiber ring cavity could be used for self-injection locking of the DFB laser and as Brillouin scattering media to generate Stokes shifted optical wave. However, a stable laser operation at two frequencies has not been reported yet preventing it from many prosperous photonic applications.

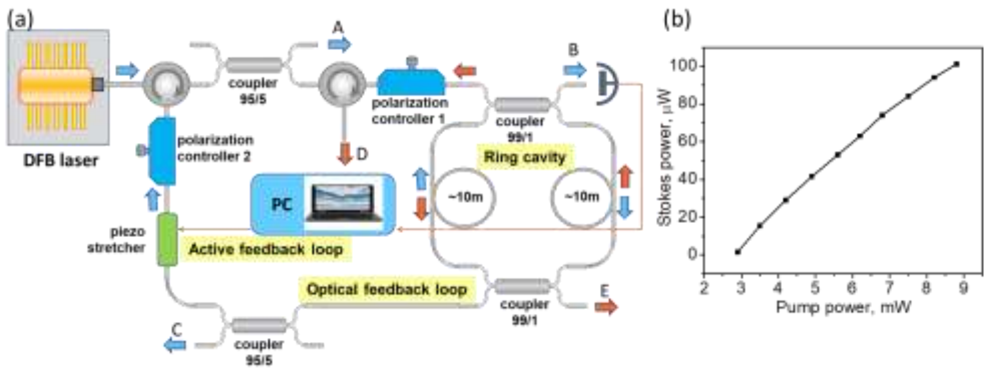

Fig. 1. (a) The experimental laser configuration; (b) Brillouin output power (port D) as a function of the DFB laser power at the fiber ring input.

It is worth noting that the fiber ring cavity is commonly used to generate Brillouin wave from an external laser diode [36-39]. However, the coupling between the DFB laser and the ring fiber cavity remains to be a technically complicated and cost consuming task [39, 40]. In this paper, we introduce a simple dual-frequency laser configuration. In our approach, the implementation of the self-injection locking mechanism into the Brillouin ring fiber laser helps to maintain coupling between the DFB laser and the external fiber cavity enabling dual-frequency laser operation. Specifically, the same ring fiber cavity is used to generate narrow-band light at the pump frequency (through self-injection locking mechanism) and narrow-band laser light at Stokes frequency (through stimulated Brillouin scattering). The system is supplied by a low-bandwidth active optoelectronic feedback circuit controlled by a low-cost USB-DAQ card that helps the laser to maintain the desired operation mode. We have explored key features of the laser performance, revealing its stability and applicability to RF harmonic generation of high spectral purity as an additional benefit of the proposed technique.

2. EXPERIMENTAL SETUP

The experimental laser configuration is shown in Fig. 1(a). The semiconductor laser we use is a commercial distributed feedback (DFB) laser diode (MITSUBISHI FU-68PDF-V520M27B) assembled within a standard 14-pin butterfly package that is coupled to the fiber ring cavity through a circulator. The DFB laser delivering ~15 mW at ~1535.6 nm is equipped with a built-in optical isolator attenuating the power of the backward radiation by ~30 dB. The built-in optical isolator eliminates the effects of uncontrollable back reflections and sets the controllable value of the feedback signal returned to the DFB laser cavity. The external ring cavity is spliced from two SMF-28 couplers (99/1) and (99/1). In order to implement the self-injection locking mechanism, the coupler redirects a part of the light circulating inside the cavity clockwise (CW) through the circulator (OC) back into the DFB laser thus providing passive feedback to the DFB laser operation. The fiber configuration is spliced from standard telecom components and placed into a foam box to reduce the influence of the laboratory environment. No additional thermal control of the box is applied.

Comparing the reported laser configuration [32] two crucial modifications have been implemented in [33] to achieve a stable dual-frequency lasing. The first modification concerns the operation of the active feedback circuit. We have implemented a piezo-control of the fiber feedback loop instead of the DFB laser current adjustment used earlier. A piezo-activator is attached to the feedback loop fiber as shown in Fig.1(a). It is driven by a low-cost USB Multifunction DAQ (National Instrument NI USB-6009) connected to a PC. The laser power detected at the output B serves as an error signal. The DAQ manages to keep it as low as possible adjusting the DAQ output voltage applied to the piezo-activator that in its turn affects the length of the optical fiber loop. With a change of the DAQ output voltage in the range 0 - 5 V, the piezo-stretcher maintains a stable laser operation in self-injection locking regime keeping the laser generated frequency locked to the ring cavity resonance peak that always slowly walks due to environment temperature fluctuations. We have found the new control mechanism to be more practical, exhibiting much better stability and reproductivity. In particular, it significantly expands the range of the laser frequency drifts acceptable for stabilized laser operation in the self-injection locking regime.

The second modification relates to the choice of the ring cavity length. We generate Brillouin laser light with the same fiber ring cavity that is already used for self-injection locking. Inside the ring the radiation of the DFB laser at ν_L propagating CW is used to pump the Brillouin wave at $\nu_S = \nu_L - \Delta_{SBS}$ generating in CCW direction, where Δ_{SBS} is the Brillouin frequency shift. Comparing our previous laser configuration [32] the ring fiber length in [33] has been increased in 5 times (up to 20 m) to decrease the Brillouin threshold. Besides, the ring cavity length has been precisely adjusted with the single-cut [41, 42] to get perfect matching between the Brillouin frequency shift $\Delta\nu_{SBS}$ and the cavity free spectrum range (FSR), so that $\Delta\nu_{SBS} = mFSR$, where m is an integer. With the perfectly adjusted fiber ring cavity active stabilization of lasing at the frequency ν_L ensures stabilization of lasing at the frequency ν_S.

For the configuration in Fig.1(a), the lasing at the locked pump frequency ν_L could be monitored through the ports A, B, C and through the ports D, E at the Brillouin frequency ν_S. The ports A and D are used as the main laser outputs. The reflected signal from the port B is detected by a fast photodetector and is used as an error signal for the active feedback operation. The ports C and E are used as control points for laser characterization. While the DFB laser operates in a free-running regime, its linewidth is estimated to be ~10 MHz, the most of the DFB laser power is reflected by the ring cavity and released through the port B. The power recorded at the port C is negligible. Self-injection-locking causes drastic narrowing the laser linewidth down to kHz range leading to a decrease of the power released through the port B and an increase of the power emitted through the port C. So, monitoring the reflected power emitted through the ports B (the error signal) allows evaluating the efficiency of the laser linewidth narrowing through the self-injection locking mechanism and helping to maintain the laser operation in the self-injection-locking regime avoiding mode-hopping. This task is assigned to the optoelectronic feedback circuit. When CW power inside the ring cavity exceeds the Brillouin lasing threshold, the contra-propagating CCW wave is emitted through the port D. Fig. 1 (b) shows the experimental dependence of the laser power emitted at the Stokes frequency and detected in port D on the laser power emitted at the pump frequency detected in port A. No power conversion to the Stokes power occurs below the pump threshold power of 2.9 mW. Above the threshold the pump-to-Stokes conversion efficiency is estimated to be ~3.3% that is well enough for some potential laser applications (e.g. Brillouin sensing).

3. RESULTS AND DISCUSSION

Fig. 2 compares the laser operation with and without the active feedback. Typical oscilloscope traces recorded with the reflected, transmitted and Brillouin powers (ports B, C, and D, respectively) without active feedback are shown in Fig. 2 (a). The observed behavior can be interpreted in terms of the laser frequency deviation from the ring cavity resonance determined by the phase shift the light acquires in the feedback loop fiber. The higher laser frequency deviation the higher error signal P_B recorded at the port B. Driven by environment noise the ring resonance frequency slowly varies in time followed by the transmitted power P_B walking between its minimal and maximal values. When approaching the minimum value, the recorded P_B keeps it for a while highlighting the laser operation in the self-injection locking regime. In this regime the laser works against the temperature fluctuations pulling the laser frequency towards the cavity resonant peak. An increase of the CW laser power circulating inside the ring above the Brillouin lasing threshold causes lasing of the contra-propagating Brillouin CCW wave at ν_S emitted through the port D. Effective conversion to the Brillouin wave limits the transmitted laser power recorded at the port D by its Brillouin threshold value. When the CW pump power inside the ring falls below the Brillouin threshold the Brillouin lasing stops and the signal P_B increases approaching its maximal value, while spontaneous noise causes mode-hopping events disturbing the laser stability and impairing the laser performance characteristics.

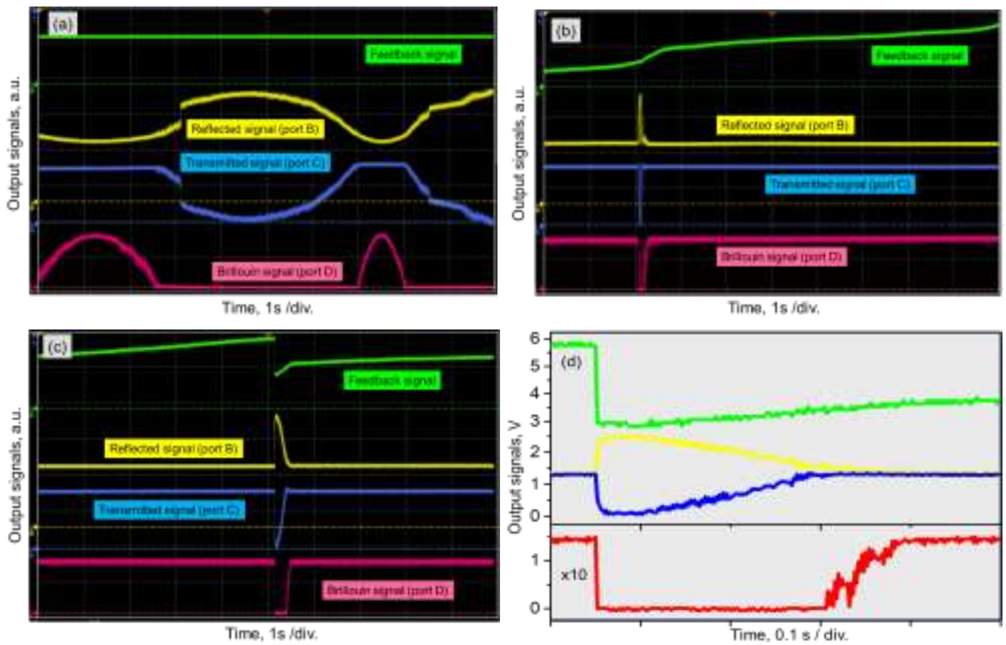

Fig. 2. Typical oscilloscope traces of the reflected (yellow curves), transmitted (blue curves) and Brillouin (red curve) optical power and active feedback control signal (green curve); (a) laser operation with optical feedback only; (b) optical and electronic feedbacks - responses on knock on the fiber ring; (c) optical and electronic feedbacks - responses on a jump of the feedback control signal; (d) a zoom of oscilloscope traces (c). The dashed lines mark zero levels.

The laser operation stabilized with the active feedback could be seen in Fig. 2 (b, c). The optoelectronic feedback circuit maintains the reflected signal recorded through port B (error signal) fixed to its minimal value. So, the DFB laser frequency is always locked to the ring cavity transmission resonant peak providing a stable laser operation at the pump and Brillouin frequencies recorded at ports A and D, respectively. One can see that all traces are almost flat exhibiting with less than ~1 % fluctuations, demonstrating that the self-injection locking mechanism in combination with optoelectronic feedback circuit perfectly works against the environment noise enabling stable laser operation at two locked frequencies.

A few experiments have been performed for characterizing the laser operation in the stabilized regime. We have determined the time constant associated with the feedback mechanism. First, we have measured the error signal response to a short pencil kick on the fiber configuration. The system response is depicted in Fig. 2 (b). When the fiber cavity is perturbed, it may exhibit a variety of dynamical behaviors. Clearly, the system behaves as a high-pass filter and so high frequency acoustic perturbations cannot be compensated by the slow acting feedback. Following these perturbations, the error signal (and the corresponding lasing frequency) makes a number of stochastic fluctuations until recoils and returns to the original point in an exponentially decaying manner. The typical time constant of the feedback mechanism is τ_P~0.2 s. The Brillouin signal is more sensitive, it stops almost immediately after a kick and starts to restore only after the complete restoration of the pump power. A typical time constant for Brillouin power restoration is much shorter τ_B~0.05 s.

Fig. 2 (c, d) shows the system response on a step change of the active feedback control signal forcing the DFB laser to switch to another mode (see a jump in electrical feedback signal). One can see that, in this case, the laser pump accepts the frequency change providing direct exponential relaxation to the new state with the same time constant of τ_P~0.2 s. Brillouin power is not generated during the whole laser transition but starts to restore with the time constant of τ_B~0.05 s immediately after. The specific features of the curves shown in Fig.2 are in good agreement with the theoretical predictions based on the self-injection locking and Brillouin lasing models [27, 38].

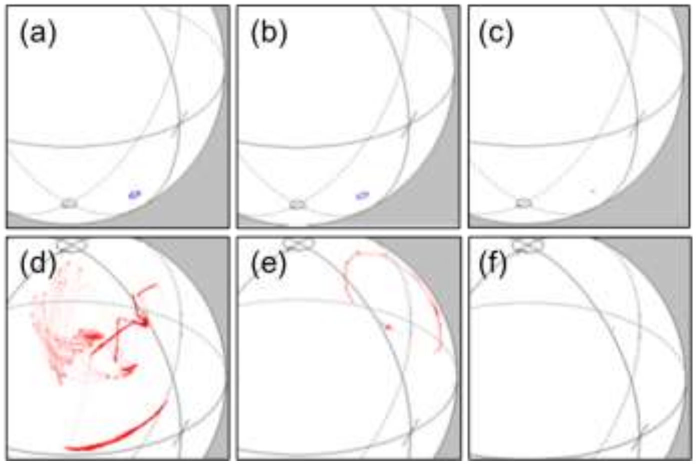

Fig. 3. Typical state of polarization trajectories on Poincare sphere for the reflected pump (port B, a-c) and Brillouin (port D, d-f) signals. (a, d) laser operation with optical feedback only; (b, e) optical and electronic feedbacks - responses on jump of the active feedback control signal; (c, f) optical and electronic feedbacks without perturbations.

To evaluate the contribution of the polarization dynamics to the stabilization of the laser operation, we use data recorded by a polarization analyzer (HP 8509A\B) from ports B, D. The polarization measurements for the laser operation without and with active feedback are shown in Fig.3. The Stokes parameters are related to the polarization attractor at the Poincaré sphere in the form of a fixed point for a few observed laser regimes. If the degree of polarization (DOP) is close to 100% then the fixed point at the Poincaré sphere indicates a stable operation. For the laser operation without the active feedback the pump wave attractor makes a precession with a small radius around a single point [Fig.3 (a)], its DOP is estimated to be ~98%. The polarization dynamics of the Brillouin signal (when it is generated) takes the form of unpredictable wandering [Fig.3 (d)]. In contrast, for the laser stabilized with the active feedback, attractors for both laser outputs are close to two fixed points of the Poincaré sphere, highlighting very high DOP estimated to be 100% [Fig.3 (c, f)]. Fig.3 also presents the polarization dynamics of the stabilized laser disturbed by the piezo-actuator (see, Fig. 2 (b, e)). During the laser restoring after a jump of the feedback control signal, the pump wave attractor exhibits behavior [Fig.3 (b)] similar to that of the laser without the active feedback [Fig.3 (a)]. It makes a precession around a single point with a small radius, its DOP is estimated to be ~97%. However, restoration of the Stokes wave is accompanied by the precession of its attractor with a rather large radius approaching the final point [Fig.3 (e)], and its DOP is estimated to be ~60%. The DOP of the pump radiation measured in the port A does not depends on the DFB laser operation mode and is always close to ~100%.

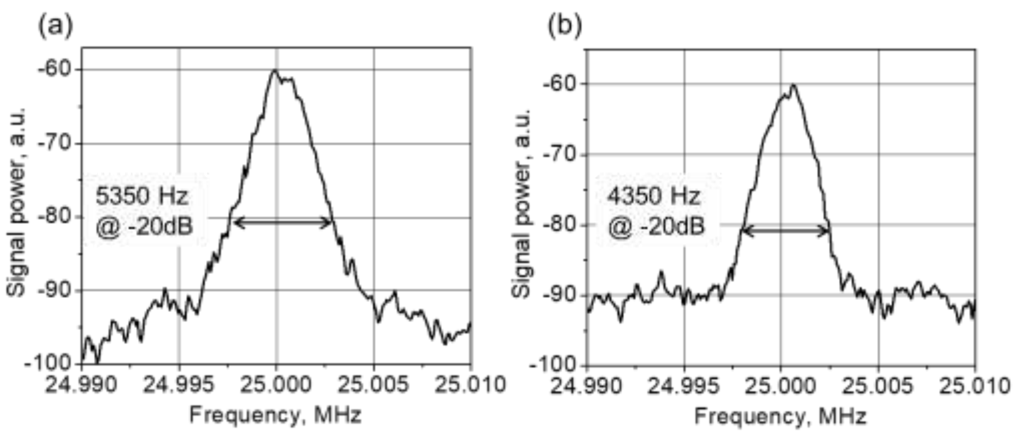

Fig. 4. Delayed self-heterodyne spectra of the laser radiation emitted through the port A at pump laser frequency (a) and the port (D) at Brillouin frequency (b).

A delayed self-heterodyne technique has been employed to measure the linewidths of radiation emitted by the stabilized laser configuration through two outputs. An all-fiber unbalanced Mach–Zehnder interferometer with a 55 km delay fiber and 25 MHz phase modulator supplied by a polarization controller is used for this purpose. The beat signal from the interferometer is detected by a ~5 GHz photodiode and analyzed by an RF spectrum analyzer (FSH8, Rohde & Schwarz). Self-heterodyne RF spectra of the stabilized laser in the pump and Brillouin channels are shown in Fig.4. The commonly used approach is that the laser full linewidth is half of the full-width half-maximum (FWHM) of the Lorentzian fit of the measured RF spectrum [43]. This estimation gives 1100 Hz and 800 Hz for the linewidths of the pump and Brillouin laser, respectively. However, more detailed analysis is required, since the laser coherence length (for both outputs) is much longer than the path difference of the interferometer [44]. (Note, for this reason, the measured spectrum features oscillations on the wings.) In a sub-coherent regime, the used method underestimates the effects of 1/f noise and overestimates the effect of the white spectrum, responsible for Gaussian and natural Lorentzian linewidths, respectively [45]. The main cause of the 1/f frequency noise in fiber lasers is temperature fluctuations induced by pump noise [46]. Since the 1/f noise is partially filtered out by the interferometer [47], we can just estimate the laser Gaussian linewidths to be between ~800 Hz and ~3kHz for both laser outputs. Here, the lower limit is determined by the measured 3-dB spectrum width (~1200Hz) with the deconvolution factor of $\sqrt{2}$ and the upper limit is set by the resolution linked to the delay fiber length. Note, the 1/f noise could be probably eliminated using low noise pumping [46]. The measured 20-dB spectrum widths are ~5350 Hz and 4350 Hz for the pump and Brillouin laser radiations. They are weakly affected by the Gaussian noise and in sub-coherent regime overestimates the FWHM Lorentzian linewidth with the deconvolution factor $2\sqrt{99}$ [48]. Therefore, the natural Lorentzian linewidth is found to be narrower than 270 Hz and 220 Hz for the pump and Brillouin laser outputs, respectively.

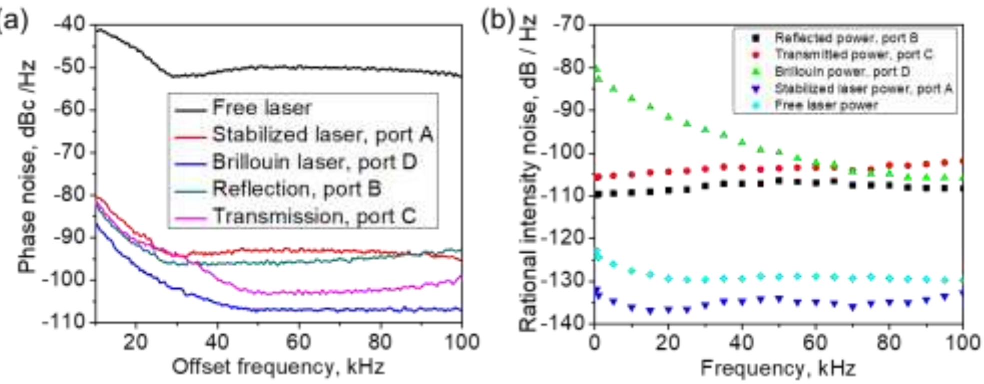

Fig. 5. Noise performance of the laser. a) Phase noise; b) Rational Intensity noise (RIN).

The noise performance of the stabilized self-injection-locked laser configuration is presented in Fig.5. Fig. 5a) depicts power spectral density (PSD) of the phase noise for the Stokes, pump, transmitted and reflected radiations measured with a spectrum analyzer (Agilent N9320A) in the radio-frequency range of 10-100 kHz. In this range the effect of the servo bandwidth of our electronic system of the laser performance is negligible. Following the method described in [49-51], the PSDs have been obtained by employing self-heterodyne technique using a fiber unbalanced Mach–Zehnder interferometer with a 1.3 km delay fiber (5.76 μs) and 20 MHz frequency shifter. One can see that active stabilization minimizes the phase noise in all measured ports. In particular, PSD measured with pump laser output (port A) is by ~ (35-40) dBc ⁄ Hz lower comparing with free-running laser. The PSD of the generated Brillouin radiation is by ~ (7-15) dBc ⁄ Hz lower comparing the pump. Due to the filtering effect of the ring cavity the pump radiation passing through the ring (transmitted and reflected) has ~ (7-15) dBc ⁄ Hz lower PSD than that measured with the direct laser output.

Fig. 5 (b) presents the relative intensity noise (RIN) measured with a lock-in amplifier SRS510 in 1-100 kHz frequency interval. One can see the RIN of the stabilized laser is lower by ~ (5 -10) dB comparing the free-running laser. At the same time, the relative intensity noise of the Stokes radiation is higher by 30-40 dB than the pump noise, especially at lower frequencies. We explain such an increase by an exponential dependence of the Brillouin wave amplification inside the fiber ring cavity on the pump wave power that is reflected in the pump-to-Stokes RIN transfer function. One can see, that the additional RIN induced by the Brillouin lasing in the fiber ring cavity is transferred into the reflected and transmitted pump RINs as well leading to their increase by 30-40 dB in respect to the stabilized pump laser wave.

Finally, the RF beating spectrum has been recorded with two laser outputs mixed in a single fiber and evaluated in terms of the peak frequency and the spectrum linewidth stabilities. A typical RF beating spectrum measured by the signal analyzer (Keysight N9040B, 50GHz) with an acquisition time of ~20 ms is shown in Fig. 6 (a). The spectrum is centered at 10946.309820 MHz that corresponds to the Brillouin frequency shift in the ring cavity fiber and exhibit a linewidth of ~290 Hz that is in good agreement with the estimations of the optical Lorentz linewidth reported above (see, Fig.3). Recording of the RF spectrum with longer acquisition time leads to its remarkable broadening due to the long-term drift of the laser frequency affected by the environmental noise. A typical RF beating spectrum acquired with averaging over ~5 min exhibits a linewidth of ~1800 Hz as shown in Fig. 6 (b). The laser operation in dual frequency mode allows us to monitor the laser frequency drift by recording the RF beat peak frequency. Indeed, the generated laser frequencies ν_L and ν_S are both the resonant ring cavity modes and so their drifts $\delta\nu_L$ and $\delta\nu_S$ relate to a change of the ring cavity optical length $\delta(nL_R)$ caused by the environmental noise. The measured deviations of the Brillouin frequency shift $\delta\nu_B = \delta\nu_L - \delta\nu_S$ is determined by the drifts of the laser frequencies $\delta\nu_L$ and $\delta\nu_S$, and so all of them are linked to $\delta(nL_R)$ as:

$$\frac{\delta\nu_L}{\nu_L} = \frac{\delta\nu_S}{\nu_S} = \frac{\delta\nu_B}{\nu_B} = -\frac{\delta(nL_R)}{nL_R} \quad (1)$$

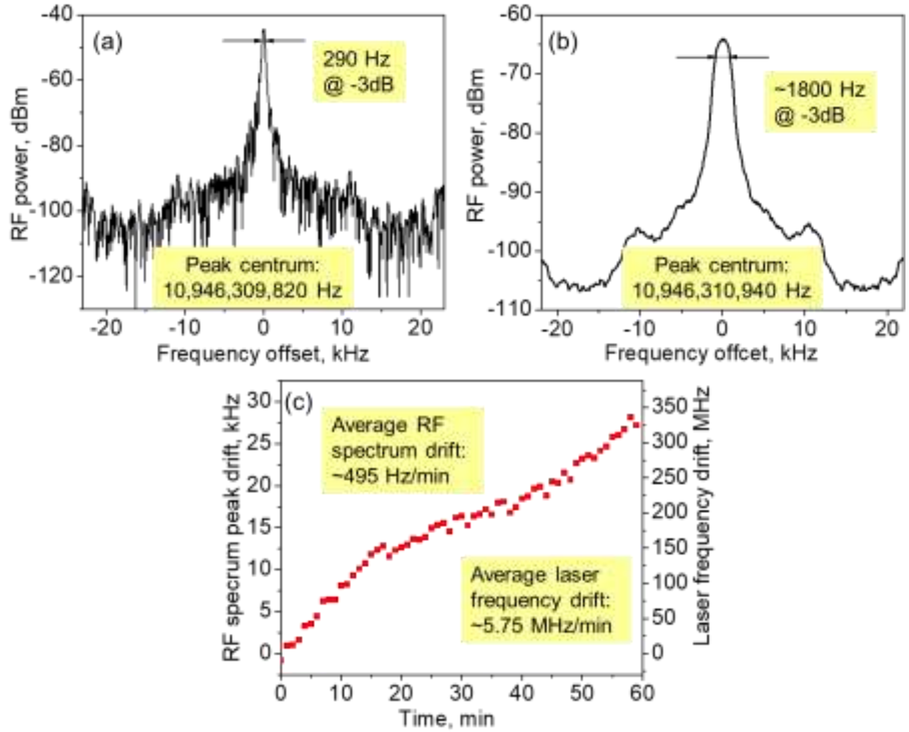

Fig. 6. RF beat spectrum evolution. a) RF beat spectrum acquired for ~20ms; b) RF beat spectrum averaged for 5 min (b) and c) evolution of the RF beat spectrum peak frequency measured each minute during 60 minutes.

Thus, the laser long-term frequency drift $\delta\nu_L = \delta\nu_B(\nu_L/\nu_B)$ is followed by the drift of the beat spectrum peak frequency $\delta\nu_B$ enabling $\delta\nu_L$ monitoring. A typical evolution of the RF spectrum peak frequency recorded during 1h (one per minute) is shown in Fig. 6 (c). One can see, it increases monotonically with a typical rate of 0.5 kHz/min passing a range of ~30 kHz. The corresponding drift of the laser frequency occurs within the range of ~300 MHz and has a typical rate of ~5.8 MHz/min that is in a good agreement with the value reported earlier under similar conditions [31]. Note, our spliced laser configuration is placed into a foam box to reduce the influence of the laboratory environment. No additional thermal control or any particular vibration and acoustics insulation protections were used.

4. CONCLUSION

In conclusion, we have introduced a simple dual-frequency laser based on a DFB laser coupled to an all-fiber ring cavity and working in self-injection-locked mode. In our laser configuration, the same ring fiber cavity is exploited both for self-injection locking of a DFB laser and for the generation of Stokes light via stimulated Brillouin scattering. A low-cost USB-DAQ is used to stabilize the system preventing mode-hopping. Importantly, a stable laser operation at two mutually locked frequencies is provided by the self-injection locking mechanism, while the active feedback loop just supports this regime. Besides, the self-injection locking mechanism maintains permanent coupling between the DFB laser and the external fiber cavity. These results enhance our understanding of the self-injection-locking mechanism in semiconductor lasers and open up new possibilities for manipulating and controlling their properties. In particular, the new ability to generate two locked frequencies is attractive for many laser applications, including high-resolution spectroscopy, phase coherent optical communications, distributed fiber optics sensing, coherent optical spectrum analyzer, and microwave photonics [52-64]. In particular, the reported laser characteristics are well superior to the requirements to the laser modules commonly used with BOTDA. In nearest future, translating the proposed laser design to integrated photonics [65-72] will dramatically reduce cost and footprint for many applications such as ultra-high capacity fiber and data center networks, atomic clocks, and microwave photonics.

ACKNOWLEDGEMENTS

The work on the laser system design and characterization was supported by the Ministry of Higher Education and Science of the Russian Federation (Megagrant Program, project # 2020-220-08-1369). The work on laser metrology and analysis of the laser frequency drift was supported by the Russian Science Foundation (project 18-12-00457).

REFERENCES

[1] Stern, B., Ji, X., Dutt, A. and Lipson, M., "Compact narrow-linewidth integrated laser based on a low-loss silicon nitride ring resonator," Opt. Lett. 42(21), 4541 (2017).

[2] Legaie, R., Picken, C. J. and Pritchard, J. D., "Sub-kilohertz excitation lasers for quantum information processing with Rydberg atoms," J. Opt. Soc. Am. B 35(4), 892 (2018).

[3] Komljenovic, T. , Davenport, M., Hulme, J. , Liu, J., Santis, C. T., Spott, A., Srinivasan, S. , Stanton, E. J. , Zhang, C. , Bowers, J. E., "Heterogeneous silicon photonic integrated circuits," Journal of Lightwave Technology 34, 20-35 (2016).

[4] Leandro, D., deMiguel-Soto, V. , López-Amo, M., "High-resolution sensor system using a random distributed feedback fiber laser," Journal of Lightwave Technology 34, 4596-4602 (2016).

[5] Shin, D. K., Henson, B. M., Khakimov, R. I., Ross, J. A., Dedman, C. J., Hodgman, S. S., Baldwin, K. G. H. and Truscott, A. G., "Widely tunable, narrow linewidth external-cavity gain chip laser for spectroscopy between 10 – 11 μm," Opt. Express 24(24), 27403 (2016).

[6] Fang, Z., Cai, H., Chen, G. and Qu, R., [Single Frequency Semiconductor Lasers], Springer Singapore (2017).

[7] Guan, H., Novack, A., Galfsky, T., Ma, Y., Fathololoumi, S., Horth, A., Huynh, T. N., Roman, J., Shi, R., Caverley, M., Liu, Y., Baehr-Jones, T., Bergman, K. and Hochberg, M., "Widely-tunable, narrow-linewidth III-V/silicon hybrid external-cavity laser for coherent communication," Opt. Express 26(7), 7920 (2018)..

[8] Yang, Z., Li, C., Xu, S. and Yang, C., [Single-Frequency Fiber Lasers], Springer Singapore (2019).

[9] Popov, S. M., Chamorovski, Y. K., Isaev, V. A., Mégret, P., Zolotovskii, I. O. and Fotiadi, A. A., "Electrically tunable Brillouin fiber laser based on a metal-coated single-mode optical fiber," Results in Physics 7, 852–853 (2017).

[10] Popov, S.M., Butov, O.V., Chamorovskiy, Y.K., Isaev, V.A., Kolosovskiy, A.O., Voloshin, V.V., Vorob'ev, I.L., Vyatkin, M.Y., Mégret, P., Odnoblyudov, M., Korobko, D.A., Zolotovskii, I.O. and Fotiadi, A.A., "Brillouin lasing in single-mode tapered optical fiber with inscribed fiber Bragg grating array," Results in Physics 9, 625–627 (2018).

[11] Popov, S. M., Butov, O. V., Chamorovski, Y. K., Isaev, V. A., Mégret, P., Korobko, D. A., Zolotovskii, I. O. and Fotiadi, A. A., "Narrow linewidth short cavity Brillouin random laser based on Bragg grating array fiber and dynamical population inversion gratings," Results in Physics 9, 806–808 (2018).

[12] Popov, S. M., Butov, O. V., Bazakutsa, A. P., Vyatkin, M. Y., Chamorovskii, Y. K. and Fotiadi, A. A., "Random lasing in a short Er-doped artificial Rayleigh fiber," Results in Physics 16, 102868 (2020).

[13] Popov, S. M., Butov, O. V., Kolosovskii, A. O., Voloshin, V. V., Vorob'ev, I. L., Isaev, V. A., Vyatkin, M. Y., Fotiadi, A. A. and Chamorovsky, Y. K., "Optical fibres and fibre tapers with an array of Bragg gratings," Quantum Electronics 49(12), 1127–1131 (2019).

[14] Spirin, V. V., López-Mercado, C. A., Mégret, P. and Fotiadi, A. A., "Single-mode Brillouin fiber laser passively stabilized at resonance frequency with self-injection locked pump laser," Laser Phys. Lett. 9(5), 377–380 (2012)..

[15] K. Petermann, *Laser diode modulation and noise* (Springer Science & Business Media, 2012).

[16] J. Ohtsubo, *Semiconductor lasers: Stability, instability and chaos* (Springer, 2012)

[17] Galiev, R. R., Pavlov, N. G., Kondratiev, N. M., Koptyaev, S., Lobanov, V. E., Voloshin, A. S., Gorodnitskiy, A. S. and Gorodetsky, M. L., "Spectrum collapse, narrow linewidth, and Bogatov effect in diode lasers locked to high-Q optical microresonators," Opt. Express 26(23), 30509 (2018).

[18] Liang, W., Ilchenko, V. S., Eliyahu, D., Savchenkov, A. A., Matsko, A. B., Seidel, D. and Maleki, L., "Ultralow noise miniature external cavity semiconductor laser," Nat Commun 6(1) (2015).

[19] Huang, S., Zhu, T., Yin, G., Lan, T., Li, F., Huang, L. and Liu, M., "Dual-cavity feedback assisted DFB narrow linewidth laser," Sci Rep 7(1) (2017).

[20] Huang, D., Tran, M. A., Guo, J., Peters, J., Komljenovic, T., Malik, A., Morton, P. A. and Bowers, J. E., "High-power sub-kHz linewidth lasers fully integrated on silicon," Optica 6(6), 745 (2019).

[21] López-Mercado, C. A., Spirin, V. V., Bueno Escobedo, J. L., Márquez Lucero, A., Mégret, P., Zolotovskii, I. O. and Fotiadi, A. A., "Locking of the DFB laser through fiber optic resonator on different coupling regimes," Optics Communications 359, 195–199 (2016)

[22] Spirin, V. V., Castro, M., López-Mercado, C. A., Mégret, P. and Fotiadi, A. A., "Optical locking of two semiconductor lasers through high-order Brillouin Stokes components in optical fiber," Laser Physics 22(4), 760–764 (2012).

[23] Spirin, V. V., López-Mercado, C. A., Mégret, P. and Fotiadi, A. A., "Single-mode Brillouin fiber laser passively stabilized at resonance frequency with self-injection locked pump laser," Laser Physics Letters 9(5), 377–380 (2012).

[24] Spirin, V. V., López-Mercado, C. A., Kinet, D., Mégret, P., Zolotovskiy, I. O. and Fotiadi, A. A., "A single-longitudinal-mode Brillouin fiber laser passively stabilized at the pump resonance frequency with a dynamic population inversion grating," Laser Phys. Lett. 10(1), 015102 (2012).

[25] Bueno Escobedo, J. L., Spirin, V. V., López-Mercado, C. A., Mégret, P., Zolotovskii, I. O. and Fotiadi, A. A., "Self-injection locking of the DFB laser through an external ring fiber cavity: Polarization behavior," Results in Physics 6, 59–60 (2016).

[26] Bueno Escobedo, J. L., Jason, J., López-Mercado, C. A., Spirin, V. V., Wuilpart, M., Mégret, P., Korobko, D. A., Zolotovskiy, I. O. and Fotiadi, A. A., "Distributed measurements of vibration frequency using phase-OTDR with a DFB laser self-stabilized through PM fiber ring cavity," Results in Physics 12, 1840–1842 (2019).

[27] Korobko, D. A., Zolotovskii, I. O., Panajotov, K., Spirin, V. V. and Fotiadi, A. A., "Self-injection-locking linewidth narrowing in a semiconductor laser coupled to an external fiber-optic ring resonator," Optics Communications 405, 253–258 (2017)..

[28] Bueno Escobedo, J. L., Spirin, V. V., López-Mercado, C. A., Márquez Lucero, A., Mégret, P., Zolotovskii, I. O. and Fotiadi, A. A., "Self-injection locking of the DFB laser through an external ring fiber cavity: Application for phase sensitive OTDR acoustic sensor," Results in Physics 7, 641–643 (2017)

[29] Spirin, V.V., Mégret, P., Fotiadi, A.A., "Passively Stabilized Doubly Resonant Brillouin Fiber Lasers," in Fiber Lasers, edited by M. Paul, J. Kolkata, INTECH 2016.

[30] Spirin, V.V., Lopez-Mercado, C. A., Mégret, P., Fotiadi, A.A. "Fiber Laser for Phase-Sensitive Optical Time-Domain Reflectometry," in Selected Topics on Optical Fiber Technologies and Applications, edited by Fei Xu and Chengbo Mou, INTECH 2018.

[31] Wei, F., Yang, F., Zhang, X., Xu, D., Ding, M., Zhang, L., Chen, D., Cai, H., Fang, Z. and Xijia, G., "Subkilohertz linewidth reduction of a DFB diode laser using self-injection locking with a fiber Bragg grating Fabry-Perot cavity," Opt. Express 24(15), 17406 (2016).

[32] Spirin, V. V., Bueno Escobedo, J. L., Korobko, D. A., Mégret, P. and Fotiadi, A. A., "Stabilizing DFB laser injection-locked to an external fiber-optic ring resonator," Optics Express 28(1), 478 (2020)..

[33] Spirin, V. V., Bueno Escobedo, J. L., Korobko, D. A., Mégret, P. and Fotiadi, A. A., "Dual-frequency laser comprising a single fiber ring cavity for self-injection locking of DFB laser diode and Brillouin lasing," Opt. Express 28(25), 37322 (2020).

[34] Hansch, T. W. and Couillaud, B., "Laser frequency stabilization by polarization spectroscopy of a reflecting reference cavity," Optics Communications 35(3), 441–444 (1980).

[35] Alnis, J., Matveev, A., Kolachevsky, N., Udem, Th. and Hänsch, T. W., "Subhertz linewidth diode lasers by stabilization to vibrationally and thermally compensated ultralow-expansion glass Fabry-Pérot cavities," Phys. Rev. A 77(5) (2008).

[36] Kotlicki, O. and Scheuer, J., "Thermal self-stability, multi-stability, and memory effects in single-mode Brillouin fiber lasers," Opt. Express 25(22), 27321 (2017).

[37] Korobko, D. A., Zolotovskii, I. O., Svetukhin, V. V., Zhukov, A. V., Fomin, A. N., Borisova, C. V. and Fotiadi, A. A., "Detuning effects in Brillouin ring microresonator laser," Optics Express 28(4), 4962 (2020).

[38] Preda, C. E., Fotiadi, A. A. and Mégret, P., "Numerical approximation for Brillouin fiber ring resonator," Opt. Express 20(5), 5783 (2012).

[39] Rossi, L. , Marini, D., Bastianini, F., Bolognini, G., "Analysis of enhanced-performance fibre brillouin ring laser for brillouin sensing applications," Opt. Express **27**, 29448-29459 (2019).

[40] Danion, G., Vallet, M., Frein, L., Szriftgiser, P. and Alouini, M., "Brillouin Assisted Optoelectronic Self-Narrowing of Laser Linewidth," IEEE Photon. Technol. Lett. 31(12), 975–978 (2019).

[41] Spirin, V. V., López-Mercado, C. A., Kablukov, S. I., Zlobina, E. A., Zolotovskiy, I. O., Mégret, P. and Fotiadi, A. A., "Single cut technique for adjustment of doubly resonant Brillouin laser cavities," Opt. Lett. 38(14), 2528 (2013).

[42] López-Mercado, C. A., Spirin, V. V., Kablukov, S. I., Zlobina, E. A., Zolotovskiy, I. O., Mégret, P. and Fotiadi, A. A., "Accuracy of single-cut adjustment technique for double resonant Brillouin fiber lasers," Optical Fiber Technology 20(3), 194–198 (2014).

[43] D. Derickson, C. Hentschel, and J. Vobis, *Fiber optic test and measurement* (Prentice Hall PTR New Jersey, 1998).

[44] Richter, L., Mandelberg, H., Kruger, M. and McGrath, P., "Linewidth determination from self-heterodyne measurements with subcoherence delay times," IEEE J. Quantum Electron. 22(11), 2070–2074 (1986).

[45] Mercer, L. B., "1 /f frequency noise effects on self-heterodyne linewidth measurements," IEEE Lightwave Technology 9, 485-493 (1991).

[46] Horak, P., Voo, N. Y., Ibsen, M., Loh, W. H.,"Pump-noise-induced linewidth contributions in distributed feedback fiber lasers," IEEE Photon. Technol. Lett. **18**, 998-1000 (2006).

[47] Horak, P. , Loh, W. H., "On the delayed self-heterodyne interferometric technique for determining the linewidth of fiber lasers," Opt Express **14**, 3923-3928 (2006).

[48] Yu, P., "A novel scheme for hundred-hertz linewidth measurements with the self-heterodyne method," Chinese Physics Letters **30**, 084208 (2013).

[49] Camatel, S. , Ferrero, V. , "Narrow linewidth cw laser phase noise characterization methods for coherent transmission system applications," Journal of Lightwave Technology **26**, 3048-3055 (2008).

[50] Llopis, O., Merrer, P. H. , Brahimi, H., Saleh, K. , Lacroix, P. "Phase noise measurement of a narrow linewidth cw laser using delay line approaches," Optics Letters **36**, 2713-2715 (2011).

[51] Li, Y., Fu, Z., Zhu, L., Fang, J. , Zhu, H., Zhong, J., Xu, P., Chen, X., Wang, J., Zhan, M., "Laser frequency noise measurement using an envelope-ratio method based on a delayed self-heterodyne interferometer," Optics Communications **435**, 244-250 (2019).

[52] Fotiadi, A. A., Antipov, O. L., & Mégret, P. (2010). Resonantly induced refractive index changes in Yb-doped fibers: the origin, properties and application for all-fiber coherent beam combining. Frontiers in Guided Wave Optics and Optoelectronics, 209-234.

[53] Boivinet, S., Lecourt, J.-B., Hernandez, Y., Fotiadi, A. A., Wuilpart, M. and Megret, P., "All-Fiber 1- μ m PM Mode-Lock Laser Delivering Picosecond Pulses at Sub-MHz Repetition Rate," IEEE Photonics Technology Letters 26(22), 2256–2259 (2014).

[54] Kuznetsov, M. S., Antipov, O. L., Fotiadi, A. A. and Mégret, P., "Electronic and thermal refractive index changes in Ytterbium-doped fiber amplifiers," Optics Express 21(19), 22374 (2013).

[55] Phan Huy, K., Nguyen, A. T., Brainis, E., Haelterman, M., Emplit, P., Corbari, C., Canagasabey, A., Kazansky, P. G., Deparis, O., Fotiadi, A. A., Mégret, P. and Massar, S., "Photon pair source based on parametric fluorescence in periodically poled twin-hole silica fiber," Optics Express 15(8), 4419 (2007).

[56] Faustov, A. V., Gusarov, A. V., Mégret, P., Wuilpart, M., Zhukov, A. V., Novikov, S. G., Svetukhin, V. V. and Fotiadi, A. A., "Application of phosphate doped fibers for OFDR dosimetry," Results in Physics 6, 86–87 (2016).

[57] Faustov, A. V., Gusarov, A., Wuilpart, M., Fotiadi, A. A., Liokumovich, L. B., Zolotovskiy, I. O., Tomashuk, A. L., de Schoutheete, T. and Megret, P., "Comparison of Gamma-Radiation Induced Attenuation in Al-Doped, P-Doped and Ge-Doped Fibres for Dosimetry," IEEE Transactions on Nuclear Science 60(4), 2511–2517 (2013).

[58] Faustov, A. V., Gusarov, A. V., Mégret, P., Wuilpart, M., Zhukov, A. V., Novikov, S. G., Svetukhin, V. V. and Fotiadi, A. A., "The use of optical frequency-domain reflectometry in remote distributed measurements of the γ-radiation dose," Technical Physics Letters 41(5), 414–417 (2015).

[59] Fotiadi, A. A., Brambilla, G., Ernst, T., Slattery, S. A. and Nikogosyan, D. N., "TPA-induced long-period gratings in a photonic crystal fiber: inscription and temperature sensing properties," Journal of the Optical Society of America B 24(7), 1475 (2007).

[60] Caucheteur, C., Fotiadi, A., Megret, P., Slattery, S. A. and Nikogosyan, D. N., "Polarization properties of long-period gratings prepared by high-intensity femtosecond 352-nm pulses," IEEE Photonics Technology Letters 17(11), 2346–2348 (2005).

[61] Kbashi, H.J., Sergeyev, S.V., Al-Araimi, M., Rozhin, A., Korobko, D., Fotiadi, A. "High-frequency vector harmonic mode locking driven by acoustic resonances," Optics Letters 44, 5112-5115 (2019).

[62] Lobach, I. A., Drobyshev, R. V., Fotiadi, A. A., Podivilov, E. V., Kablukov, S. I. and Babin, S. A., "Open-cavity fiber laser with distributed feedback based on externally or self-induced dynamic gratings," Opt. Lett. 42(20), 4207 (2017).

[63] Korobko, D. A., Fotiadi, A. A. and Zolotovskii, I. O., "Mode-locking evolution in ring fiber lasers with tunable repetition rate," Opt. Express 25(18), 21180 (2017).

[64] Lobach, I. A., Kablukov, S. I., Podivilov, E. V., Fotiadi, A. A. and Babin, S. A., "Fourier synthesis with single-mode pulses from a multimode laser," Opt. Lett. 40(15), 3671 (2015).

[65] Eggleton, B. J., Poulton, C. G., Rakich, P. T., Steel, M. J., Bahl, v, "Brillouin integrated photonics," Nature Photonics, 1-14 (2019).

[66] Diamandi, H. H., Zadok, A., "Ultra-narrowband integrated brillouin laser," Nature Photonics **13**, 9-10 (2019).

[67] Gundavarapu, S. , Brodnik, G. M., Puckett, M., Huffman, T., Bose, D. , Behunin, R., Wu, J., Qiu, T., Pinho, C. , Chauhan, N. , Nohava, J., Rakich, P. T., Nelson, K. D., Salit, M., Blumenthal, D. J., "Sub-hertz fundamental linewidth photonic integrated brillouin laser," Nature Photonics **13**, 60-67 (2019).

[68] Mirnaziry, S. R., Wolff, C., Steel, M. J., Eggleton, B. J., Poulton, C. G. , "Stimulated brillouin scattering in integrated ring resonators," J Opt Soc Am B **34**, 937-949 (2017).

[69] Otterstrom, N. T., Behunin, R. O. , Kittlaus, E. A., Wang, Z. , Rakich, P. T. , "A silicon brillouin laser," Science **360**, 1113-1116 (2018).

[70] Morrison, B., Casas-Bedoya, A., Ren, G. , Vu, K., Liu, Y., Zarifi, A., Nguyen, T. G., Choi, D.-Y., Marpaung, D. , Madden, S. J., "Compact brillouin devices through hybrid integration on silicon," Optica **4**, 847-854 (2017).

[71] Marpaung, D. , Yao, J. , Capmany, J., "Integrated microwave photonics," Nature Photonics **13**, 80-90 (2019).

[72] Li, J., Suh, M.-G., Vahala, K., "Microresonator brillouin gyroscope," Optica **4**, 346-348 (2017).